

Theoretical Calculations and Matrix-Isolation FT-IR Studies of Hydrogen-Bonded Complexes of Molecules Modeling Cytosine or Isocytosine Tautomers. 7. 2-Hydroxypyridine/2-Oxopyridine Complexes with H₂O

Ahmed Dkhissi,[†] Linda Houben,[†] Johan Smets,[†] Ludwik Adamowicz,[‡] and Guido Maes^{*,†}

Department of Chemistry, University of Leuven, Celestijnenlaan 200F, B3001 Heverlee, Belgium and
Department of Chemistry, University of Arizona, Tucson, Arizona 85721

Received: April 4, 2000; In Final Form: July 18, 2000

The H-bond interaction between the tautomeric cytosine-modeling system, 2-hydroxypyridine (2HP)/2-oxopyridine (2OP), with water is investigated using matrix-isolation FT-IR spectroscopy and ab initio calculations performed with the RHF and MP2 methods and the DFT method with the B3-LYP hybrid functional. Equilibrium structures of six different complexes have been found in the calculations. The theoretical results indicate that the closed N···H–O···H–O and C=O···H–O···H–N H-bonded water complexes are the most stable systems for the 2HP and the 2OP tautomers, respectively. Both closed complexes as well as the three open complexes O–H···OH₂, N···H–OH, and C=O···H–OH have been identified in the experimental spectrum. A detailed analysis of the structural, energetic and vibrational parameters for the closed complexes has been performed. Both in the matrix (Ar) and in the gas phase, the hydroxy tautomer, 2HP, is more stable than the oxo form, 2OP. An important observation is that addition of a single water molecule shifts the tautomeric equilibrium toward the oxo 2OP form, which is in agreement with the theoretical calculations.

Introduction

The tautomerism of 2-hydroxypyridine/2-oxopyridine has been studied by a great variety of methods. In our previous paper devoted to the study of the water-induced tautomeric shift for 2-OH-pyrimidine and 5-Br-2-OH-pyrimidine, we have recalled the most notable of these papers (refs 14–27 in ref 1). In the former papers of this series,^{1–6} we have demonstrated that coupling the matrix-isolation FT-IR to ab initio computational methods is one of the most suitable approaches for evaluating the intrinsic tautomeric and H-bonding characteristics of poly-functional bases. This approach has allowed a detailed description of the tautomeric and H-bonding behavior of cytosines.^{1–6} In some of these previous studies, only a single tautomer of the studied base was present in low-temperature Ar matrices,^{2–5} while in other cases the presence of several tautomeric forms was detected in the matrices.^{1,6}

In continuing the line of study, which has included investigations of 2-OH-pyrimidine·H₂O¹ and 1-CH₃-cytosine·H₂O,⁶ we consider in the present work the H-bond interaction of 2-OH-pyridine and its tautomer 2-oxopyridine with water in Ar matrices. In the former reports, all calculations have been performed using ab initio methods. In this work we have also applied this approach, but we have also used the DFT (density functional theory method). The results of the DFT(B3-LYP)/6-31++G** calculations are compared with the results obtained from RHF/6-31++G** and MP2//RHF/6-31++G** methods and with experimental data of matrix isolation FT-IR and of the gas-phase measurements. Held and Pratt⁷ reported the gas-phase structures of 2OP·H₂O in its S₀ and S₁ electronic states. Their analysis was based on the rotationally resolved S₁ ← S₀

fluorescence excitation spectra of the mono- and disolvated water complexes of 2OP. Their results are very useful to evaluate the level of theory required to reliably describe structural properties for hydrogen-bonded complexes. Furthermore, Matsuda et al.⁸ recently measured the three vibrational modes $\nu^{\text{b}}_{\text{OH}}$, ν_{NH} , and $\nu_{\text{C=O}}$ of the closed H-bonded 2-oxopyridine–H₂O system in the supersonic jet. These frequencies will be used here to support the proposed assignment of the complicated IR spectrum of 2HP/2OP–H₂O.

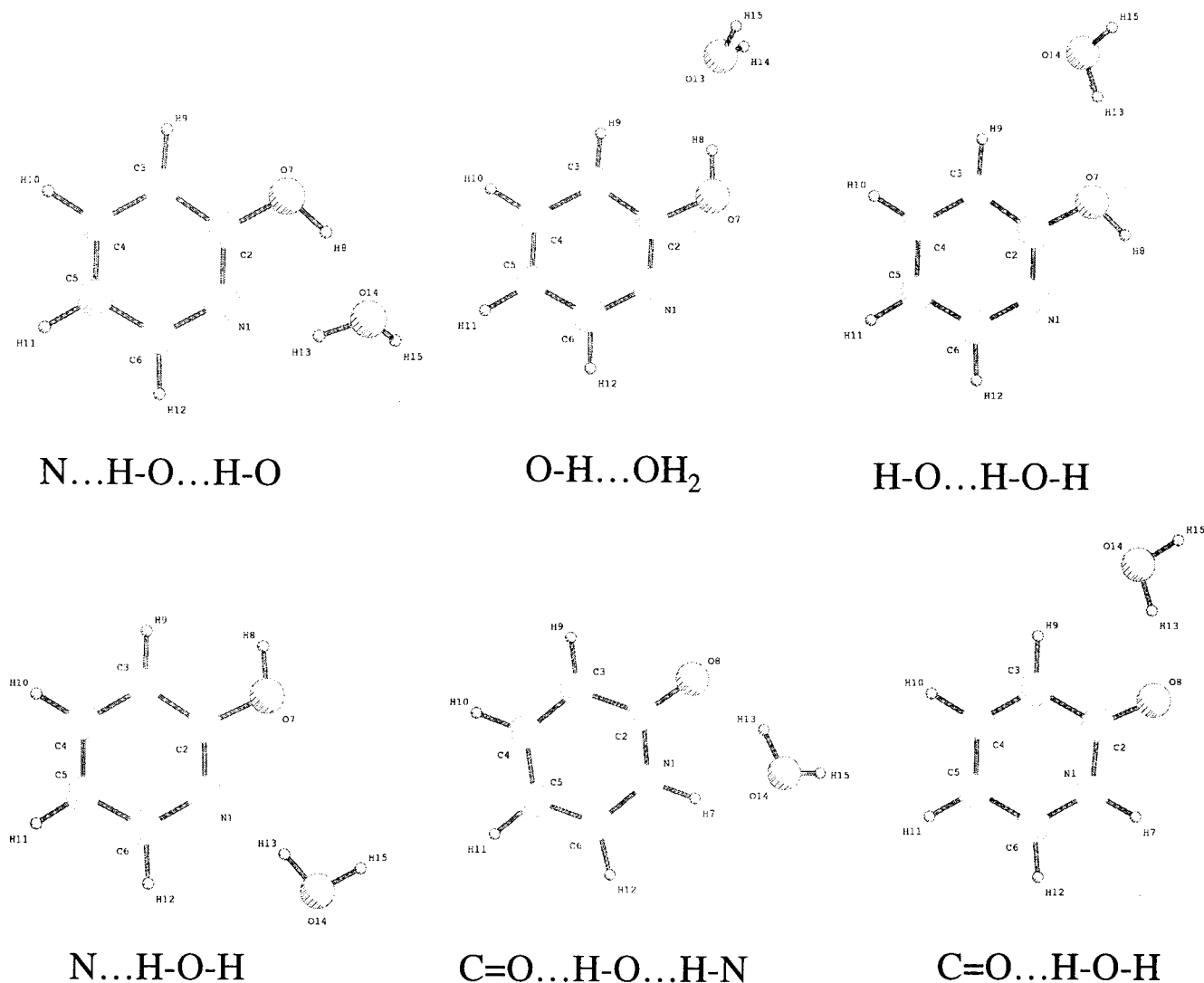
Contrary to the 2-OH-pyrimidine/2-pyrimidone system, where the hydroxy form predominates in a low-temperature matrix,⁹ 2-OH-pyridine occurs in comparable amounts as the hydroxy and oxo tautomers.^{10–12} Similarly to several cytosine derivatives,^{13–15} the presence of the two (or more) tautomeric forms in comparable amounts complicates the spectral assignment of the experimental absorptions, especially when the water complexes of all these tautomers have to be considered.

A variety of experimental measurements, including those done by UV and IR spectroscopies,¹⁶ X-ray spectroscopy,¹⁷ UV photoelectron spectroscopy¹⁸ and IR spectroscopy in inert-gas matrices,¹¹ and microwave spectroscopy¹⁹ have indicated that the free energy difference between the hydroxy 2HP and the oxo 2OP forms is 2–4 kJ·mol^{–1} in favor of the hydroxy form. Polar solvents induce transition from the hydroxy to the oxo form (by stabilizing the oxo form by about 4 kJ·mol^{–1}) through a double proton-transfer process.^{9b,20} The shift of the tautomeric equilibrium induced by the polar environment is usually explained by the larger dipole moment of the oxo form and by its ability to form stronger H-bonds with one or more solvent molecules.

In this work, we describe both experimental spectral and computational results for the interaction between water and 2HP/2OP. Both tautomers have several groups available for the

[†] University of Leuven.

[‡] University of Arizona.

CHART 1: Structures of the Complexes Considered in This Work

H-bonding with water. It is therefore desirable to first investigate all possible isomeric 1:1 H-bonded complexes with quantum-mechanical calculations. Six minima on the potential energy surfaces of the 2HP/2OP·H₂O complexes (Chart 1) have been found in the calculations, and their relative energies have been obtained. The theoretical results demonstrate that the closed H-bonded complexes containing two H-bonds are the most stable structures, which is consistent with the experimental results. For these complexes, a detailed structural analysis and spectral assignments have been performed.

Methodology

Theoretical Methodology. Geometries and vibrational frequencies of the complexes were calculated using the Becke three-parameter hybrid functional²¹ combined with the Lee, Yang, and Parr correlation functional.²² This method has been shown to produce more reliable rotational constants, geometries, and vibrational frequencies for hydrogen-bonded systems involving the DNA bases than obtained with other functionals.^{23,24} On the other hand, this does not imply that more extended ab initio methods such as MP2 or CCSD(T) would not yield even more accurate results. For instance, the shift of the OH stretching frequency of the H-bonded proton-donor molecule is best predicted with the DFT/B3-LYP method. Therefore this approach was selected for the study of 2HP/2OP

complexed with H₂O. Furthermore, to allow a comparison with other H-bonded systems studied by high-level ab initio calculations and experimental matrix-isolation vibrational spectroscopy, optimized geometries as well as IR frequencies and intensities of all the complexes obtained in the DFT calculations have also been determined at the RHF level of theory. For the RHF optimized molecular structures calculations of the total energies of the complexes were performed with the MP2 method.

For the molecular orbital expansion we have used the 6-31++G** basis set. The choice of this basis set was based on the consideration that, to obtain reliable properties for hydrogen-bonded systems, it is essential to employ a basis set that possesses sufficient diffuseness and angular flexibility.²⁵ This basis set has been sufficient to predict reliable structural and vibrational properties for hydrogen-bonded systems in our earlier studies.²³

The computed total energy for each system includes the zero-point vibrational energy (ZPE) calculated using the DFT and MP2 methods and the harmonic approximation. The ZPE's were scaled down using a scaling factor of 0.970 and 0.960, respectively. For the closed complexes, the BSSE correction has also been applied in this study. The IR frequencies and intensities were also computed at the RHF and DFT levels of theory using analytical derivative procedures implemented in the Gaussian 94 program.²⁶

TABLE 1: 2-Hydroxypyridine (2HP)/2-Oxopyridine (2OP) and Their H-Bonded Complexes with Water: Total Energies (au), Relative Energies (kJ·mol⁻¹), H-Bond Energies (kJ·mol⁻¹), and Dipole Moments (D) Calculated with the 6-31++G Basis Set**

	2HP	N···HO···H-O	HO···HOH	O-H···OH ₂	N···HOH	2OP	CO···HO···H-N	CO···HO-H
E	MP2 -322.5924 063	-398.8418 285	-398.8340 038	-398.8301 365	-398.8282 607	-322.58 80084	-398.84 04982	-398.83 44747
	DFT -323.5438 012	-399.9945 626	-399.9851 286	-399.9817 756	-399.9803 038	-323.54 45169	-399.99 75033	-399.99 15241
ZPE ^a	MP2 0.0903033	0.1143840	0.1131869	0.1133045	0.1130859	0.09053 12	0.11456 67	0.11392 64
	DFT 0.0905757	0.1150420	0.1135375	0.1136927	0.1134376	0.09072 701	0.11509 54	0.11433 20
ET	MP2 -322.5021 030	-398.7274 445	-398.7208 169	-398.7168 320	-398.7151 748	-322.49 74772	-398.72 59315	-398.72 05483
	DFT -323.4532 255	-399.8795 206	-399.8715 911	-399.8680 829	-399.8668 662	-323.45 37899	-399.88 24079	-399.87 71921
ΔE ^b	MP2	0.00	17.40	27.86	32.21		0.00	14.13
	DFT	0.00	20.82	30.03	33.22		0.00	13.69
ΔE ^c	MP2	0.00	17.40	27.86	32.21		3.97	18.10
	DFT	7.58	28.40	37.61	40.80		0.00	13.69
H-bond energy	MP2	-44.34 (-27.77) ^d	-23.80	-37.76	-32.83		-52.40 (-36.11)	-36.58
	DFT	-43.68 (-33.50)	-18.91	-33.53	-29.67		-49.52 (-36.41)	-33.83
μ(D)	MP2	1.53	2.76	1.66	5.04	4.81	3.36	5.22
	DFT	1.46	2.78	1.46	5.05	4.59	3.54	5.07

^a Calculated as $0.90\Sigma\nu_i$ for RHF and $0.97\Sigma\nu_i$ for DFT. ^b Energy difference between isomeric complexes of the same tautomer. ^c Energy difference with the most stable complex. ^d Numbers in parentheses correspond to the H-bond energy corrected with ZPE and BSSE.

Finally, potential energy distributions (PED's) have been calculated and the predicted IR frequencies were scaled to account for various systematic errors in the theoretical approach. Two scaling procedures were applied. In the first applied to the RHF frequencies, all frequencies were scaled with a uniform scaling factor of 0.900, and in the second applied to the DFT frequencies, scaling was performed with a set of different scaling factors (reflecting the difference in anharmonicity) depending on the different types of the vibrational modes, i.e., 0.950 for $\nu(\text{XH})$, 0.980 for the out-of-plane modes, and 0.975 for all other modes. The use of different scaling factors for frequencies of different types of vibrational modes was proposed by other authors.²⁷⁻³⁰

Experimental Methodology. The solid compound 2-OH-pyridine with the purity of 97% was obtained from ACROS. The matrix gas Ar (99.9999%) was purchased from UCAR. Ar/H₂O mixtures at variable *M/S* ratios (100–500) were prepared in a glass vacuum line. The Bruker IFS88 FT-IR instrument and the low-temperature cryogenic equipment used in the experiments were already described in our earlier papers.^{31,32} The optimal sublimation temperature for 2-OH-pyridine was 303 K. Annealing of the matrixes was performed at 35–39 K during 5–10 min.

The OD-deuterated compound was prepared by dissolving the OH compound in CH₃OD (Aldrich, 99%) and recrystallization under the N₂ atmosphere. This was repeated four times, and the OD content of the final deuterated compound was ±95%. The 2OD-pyridine/H₂O/Ar matrixes were prepared similar to the 2OH-pyridine/H₂O/Ar matrixes.

Results and Discussion

Energetic and Structural Properties. We have theoretically analyzed four possible 1:1 H-bonded complexes of water with 2HP and two possible complexes of water with 2OP (Chart 1). The total MP2/6-31++G** and DFT(B3-LYP)/6-31++G** energies and the H-bond interaction energies of all the isomeric complexes obtained in the calculations are summarized in Table 1.

Upon analyzing the results, we first note that the interaction energies for 2HP/2OP·H₂O are smaller than those obtained for the interaction of 2HP/2OP with hydrogen chloride,³³ which can be explained by a stronger proton-donor character of HCl than of H₂O.

Among the four isomeric complexes of 2HP, the N···H-O···H-O structure (Chart 1) is the most stable one at both MP2 and DFT/B3-LYP levels of theory. Moreover, the order of

TABLE 2: Experimental and Computed Rotational Constants (MHz) for Closed H-Bonded Complexes of 2-Oxopyridine and 2-Hydroxypyridine with H₂O Calculated with the 6-31++G Basis Set**

	RHF	B3-LYP	expt ^a
2-Oxopyridine-H ₂ O			
A	4053	3984	3997
B	1350	1397	1394
C	1013	1034	1035
mean dev	41	6	
2-Hydroxypyridine-H ₂ O			
A	4053	3991	
B	1357	1417	
C	1019	1048	

^a Taken from ref 7.

stability of the four structures is the same for MP2 and B3-LYP methods. For the two water complexes of 2OP, the C=O···H-O···H-N structure is the most stable one. The difference in the interaction energies between the closed and open complexes reflects the cooperative effect of the two H-bonds in the closed complexes. This effect was analyzed previously for the 2-hydroxypyrimidine-H₂O complexes.¹ Another important result emerging from the theoretical calculations is that the H-bond energies (ZPE and BSSE corrected) for the two closed complexes are -27.77 (MP2) or -33.50 kJ·mol⁻¹ (DFT) for 2HP-H₂O and -36.11 (MP2) or -36.41 kJ·mol⁻¹ (DFT) for 2OP-H₂O. These results indicate that 2OP interacts more strongly with a single water molecule than 2HP. This is consistent with other theoretical data^{34,35} and with 2OP being the more stable tautomer than 2HP in polar solvents due to its larger dipole moment (4.26 D).

The difference in the relative energy, ΔE, between the closed structures, N···H-O···H-O and C=O···H-O···H-N, is 3.97 kJ·mol⁻¹ in favor of the hydroxy form at the MP2 level but 7.58 kJ·mol⁻¹ in favor of the oxo form at the DFT level. Similar discrepancies between ΔE values computed using ab initio and DFT methods have been found for 2-thio-HP/2-thio-OP³⁶ and for cytosine or thio- and selenocytosine.³⁷

Table 2 collects the rotational constants calculated with different methods (RHF, DFT), as well as the experimental data when available. The mean deviations for the predicted rotational constants of 2OP-H₂O are 41 and 6 MHz for RHF and DFT/B3-LYP, respectively. It was determined that B3-LYP/6-31++G** reproduces better the experimental rotational constants than B3-LYP/SVP³⁵ and MP2/6-31+G**. The overall quality of the B3-LYP method is confirmed by the present comparison. In Table 3, we have collected selected structural

TABLE 3: Selected Structural Data for Closed H-Bonded Complexes of 2-Oxopyridine and 2-Hydroxypyridine with H₂O^a

	RHF	B3-LYP	expt ^b
2-Oxopyridine–H ₂ O: O ₁₄ –H ₁₃ ···O ₈ Bond			
<i>R</i> (O ₁₄ O ₈)	2.828	2.722	2.77
<i>r</i> (O ₁₄ H ₁₃)	0.953 (0.010) ^c	0.986 (0.021)	
<i>r</i> (O ₁₄ H ₁₅)	0.942 (0.001)	0.964 (0.001)	
<i>r</i> (C ₂ =O ₈)	1.216 (0.010)	1.246 (0.014)	
∠(H ₁₃ O ₁₄ O ₈)	23	20	
∠(O ₈ H ₁₃ O ₁₄)	145	150	139.6
2-Oxopyridine–H ₂ O: N ₁ –H ₇ ···O ₁₄ Bond			
<i>R</i> (N ₁ O ₁₄)	2.974	2.839	2.86
<i>r</i> (N ₁ H ₇)	1.002 (0.005)	1.025 (0.012)	
<i>r</i> (N ₁ C ₂)	1.374 (0.007)	1.400 (0.011)	
∠(H ₇ N ₁ O ₁₄)	24	23	
∠(N ₁ H ₇ O ₁₄)	144	145	146.2
2-Hydroxypyridine–H ₂ O: N ₁ ···H ₁₃ –O ₁₄ Bond			
<i>R</i> (N ₁ O ₁₄)	2.94	2.77	
<i>r</i> (O ₁₄ H ₁₃)	0.951 (0.008)	0.985 (0.020)	
<i>r</i> (O ₁₄ H ₁₅)	0.943 (0.000)	0.965 (0.000)	
<i>R</i> (N ₁ C ₂)	1.313 (0.005)	1.340 (0.010)	
∠(N ₁ H ₁₃ O ₁₄)	136	143	
2-Hydroxypyridine–H ₂ O: O ₇ –H ₈ ···O ₁₄ Bond			
<i>R</i> (O ₇ O ₁₄)	2.88	2.75	
<i>R</i> (O ₇ H ₈)	0.953 (0.007)	0.987(0.016)	
<i>r</i> (C ₂ =O ₇)	1.326 (0.009)	1.343 (0.014)	
∠(O ₇ H ₈ O ₁₄)	163	161	

^a Distances are in Å, and angles, in deg. ^b Reference 7. ^c The elongation of the bond length upon complexation.

properties calculated with different methods and experimental data, if available, for the two closed complexes 2OP–H₂O and 2HP–H₂O. In the first instance, the intermolecular distances calculated with the RHF method are much larger than those obtained from the experiment,⁷ for both complexes. This difference must be attributed to the electron correlation effects, which are not accounted for in the RHF method. Furthermore, for the 2OP–H₂O complex, B3-LYP yields results in good agreement with the available MP2 calculations³⁸ and with the experimental results. For instance, the B3-LYP/6-31++G** *R*(O₁₄–O₈) distance of 2.722 Å is slightly shorter than the MP2 result (2.75 Å) and the experimental distance (2.77 Å), while the *R*(N₁–O₁₄) distance is in a good agreement with both the MP2 (2.839 versus 2.840 Å, for B3-LYP and MP2, respectively) and the experimental data (2.86 Å). For 2HP–H₂O, neither MP2 nor experimental data are available and a direct comparison with our results is not possible.

Both RHF and B3-LYP methods predict intermolecular angles, ∠(O₈–H₁₃–O₁₄) and ∠(N₁–H₇–O₁₄), in good agreement with the experimental data (see Table 3). The H-bond angles, ∠(N₁–H₁₃–O₁₄) and ∠(O₇–H₈–O₁₄), calculated with RHF are similar to the angles in the closed complex of water-2-hydroxypyrimidine but noticeably smaller than the similar angles in the open complexes of pyridine–H₂O² and 4-OH-pyridine–H₂O.⁴ Thus, the two H-bonds in the closed complex are far from the “perfect”, linear H-bond. As for 2-hydroxypyrimidine complexed with water,¹ the distortion from the perfect alignment also in this case reduces the H-bond cooperativity.

One of the most interesting structural quantities is the elongation of the X–H bond due to the H-bonding, since this effect is the key for a reliable interpretation (X–H frequency shift) of the IR vibrational spectra of the hydrogen-bonded complexes. The elongation of the X–H bond calculated with RHF in this work is considerably smaller than the value obtained with the B3-LYP functional. This result suggests that the RHF Δ*ν*_{X–H} frequency shift would be smaller than that obtained with

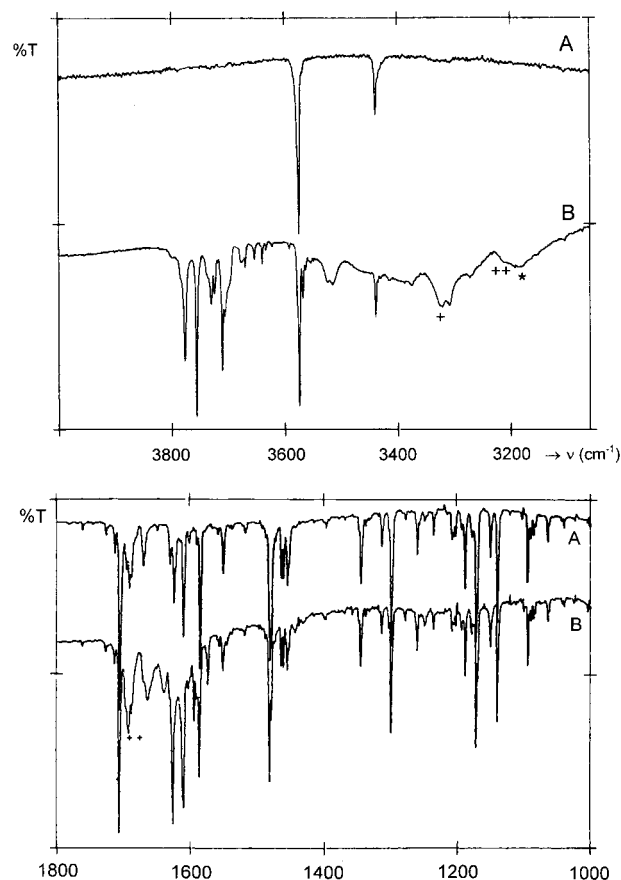


Figure 1. FT-IR spectrum of an Ar-matrix doped with 2HP/2OP and H₂O: (A) 2HP/2OP in Ar; (B) 2HP/2OP/H₂O in Ar; †, new H₂O absorption from the hydroxy complex; ††, new H₂O absorption from the oxo complex; +, new base vibration of the hydroxy tautomer; ++, new base vibration of the oxo tautomer; *, dimer of 2HP/2OP.

the DFT method, and this indeed is the case. The same observation has been made for 2HP–HCl and 2OP–HCl complexes.³³ The largest changes in the X–H bond length due to the H-bond formation are the increase of 0.012 Å (DFT) of the N₁–H₇ bond in 2OP–H₂O and the increase of 0.016 Å (DFT) of the O₇–H₈ bond for 2HP–H₂O. We attribute these relatively large changes to the cooperativity effect in the closed complexes.

Spectral Properties. 2-Hydroxypyridine occurs as a hydroxy/oxo tautomeric mixture in Ar matrixes, with a tautomerization constant, *K*_T(oxo/hydroxy), varying from 0.36 to 0.46.^{11,39} As a matter of fact, the IR spectrum of the matrix-isolated compound is rather complicated as it exhibits intense *ν*_{OH}, *ν*_{NH}, and *ν*_{C=O} absorptions, as well as a very rich fingerprint pattern.^{11,39}

Figure 1 illustrates the complicated FT-IR spectrum of 2HP/2OP in the presence of water in Ar. Apart from the bands originating from free H₂O or from the two free tautomers of the base, many new absorption bands are found to be H₂O-induced: new bands in the *ν*₃ (H₂O) region at 3706, 3700, 3696, and 3690 cm⁻¹; to new, intense absorptions at 3330 and 3308 cm⁻¹; a weak absorption at 3524 cm⁻¹, close to the water trimer band; a rather weak and narrow band at 3414 cm⁻¹; a weak band at 3270 cm⁻¹; a broader band at 3210 cm⁻¹; two shifted *ν*_{C=O} bands at 1694 (–10) and 1691 (–13) cm⁻¹; a shifted (+6) *γ*_{C=O} component at 769 cm⁻¹; a shifted (–5) *ν*_{OH}(2HP) mode at 3568 cm⁻¹.

This complicated spectral pattern must be related to the formation of H-bonded complexes of the two tautomers. We will describe the assignment of the bands separately for the 2OP and 2HP complexes.

2OP Complexes. The observation that $\nu_{\text{C=O}}$ shifts downward and $\gamma_{\text{C=O}}$ shifts upward indicates that the C=O group acts as a proton acceptor. The frequency shift of the band at 1694 cm^{-1} (shifted by -10 cm^{-1}) is of the same order of magnitude as the $\Delta\nu_{\text{C=O}}$ values found for uracils H-bonded to H_2O in Ar.⁴⁰ Since the shift of ν_3 is $3706 \rightarrow 3704\text{ cm}^{-1}$ and for $\nu^{\text{b}}\text{OH}$ is $3530 \rightarrow 3513\text{ cm}^{-1}$ for uracils-water,⁴⁰ we assign the ν_3 and $\nu^{\text{b}}\text{OH}$ modes for 2OP- H_2O to the absorptions at 3706 and 3524 cm^{-1} , respectively. These results indicate that an open H-bonded structure with H_2O is present in Ar. After correction for the decreased coupling in the bonded H_2O molecule,⁴¹ and when the calculated $\text{PA}_{\text{C=O}}$ value of 898 kJ/mol ⁴² is used for 2OP, the corrected $\nu^{\text{b}}\text{OH}$ frequency (3544 cm^{-1}) yields the relative $\Delta\nu^{\text{b}}\text{OH}$ shift which correlates well in the C=O bases diagram.⁴¹

The second new $\nu_{\text{C=O}}$ band with a decreased frequency of 1691 cm^{-1} suggests that another, stronger complex of the 2OP tautomer with H_2O is also present. The rather strong intensity increase of this $\nu_{\text{C=O}}$ absorption indicates that the abundance of the oxo tautomeric form increases when the matrix 2HP/Ar is doped with water. This is in accordance with the theoretical predictions (Table 1). Since the H_2O molecule in the closed $\text{C=O}\cdots\text{H}-\text{O}\cdots\text{H}-\text{N}$ structure is expected to be strongly perturbed,⁴³ the bands observed at 3270 and at 3210 cm^{-1} can be assigned to the $\nu^{\text{b}}\text{OH}$ and ν_{NH} modes respectively in this structure. The first supporting argument is that the $\nu^{\text{b}}\text{OH}$ mode of the closed H-bonded complex is expected to be a rather broad absorption, as was the case for 2-pyrimidone- H_2O .¹ The frequency 3270 cm^{-1} yields a relative shift of about 0.12, which is situated far above the correlation curve of $\Delta\nu/\nu$ versus $\text{PA}_{\text{C=O}}$ for the $\text{C=O}\cdots\text{H}-\text{OH}$ systems.⁴¹ The shift of -228 cm^{-1} for the base N-H mode is not unusual for such a strong complex, since shifts of $-120 \rightarrow -180\text{ cm}^{-1}$ have been observed for open $\text{N}-\text{H}\cdots\text{OH}_2$ complexes of uracils in Ar.⁴⁰ The $\nu^{\text{f}}\text{OH}$ mode of this closed complex is probably contributing to the absorption around 3700 cm^{-1} . As it is well-known, the H-bond cooperativity effect occurs in systems with two or more H-bonds at the same or closely neighboring proton-donor or proton-acceptor sites.⁴⁴ A suitable method to evaluate the H-bond cooperativity is to compare the frequency shift, $\Delta\nu_{\text{OH}}$, for the bridged AH bond in $\text{A}-\text{H}\cdots\text{A}-\text{H}\cdots\text{B}$ with the frequency shift of the AH bond in the 1:1 $\text{A}-\text{H}\cdots\text{B}$ complex.⁴⁵ Comparison of the corrected shifts for the bonded water mode in the open and in the closed complex of the 2OP tautomer yields a cooperativity A_{b} value of 2.57. This value indicates a substantial cooperativity effect, since for the linear 1:2 $\text{B}\cdots\text{H}-\text{O}\cdots\text{HO}$ water complexes the average ratio of the cooperativity factor A_{b} is 1.37.⁴⁵

Matsuda et al.⁸ have assigned the $\nu^{\text{f}}\text{OH}$, $\nu^{\text{b}}\text{OH}$, ν_{NH} , and $\nu_{\text{C=O}}$ modes for the closed 2-oxopyridine- H_2O complex to the frequencies 3725 , 3346 , 3329 , and $1707/1699\text{ cm}^{-1}$, respectively. Comparison with the assignments proposed above indicates that the $\Delta\nu^{\text{b}}\text{OH}$ and $\Delta\nu_{\text{NH}}$ values are somewhat larger in the matrix. This is due to the well-known effect of matrix fortification.^{33,46} However, the assignment of the $\nu^{\text{f}}\text{OH}$ mode at 3725 cm^{-1} seems to be questionable, since this mode is already at 3711 cm^{-1} for the weaker water dimer and some unassigned bands are present in the region $3700-3690\text{ cm}^{-1}$ in the spectrum published by Matsuda et al.⁸

2HP Complexes. The remaining new absorption bands are due to H-bonding between 2-hydroxypyridine and H_2O , either at the N atom or at the OH group of the base or simultaneously at both sites. The question again arises whether both open and closed complexes of the hydroxy tautomer are present. The theoretical energy calculations shown in Table 1 predict the

closed complex to be the more stable one, even lower in energy than the closed structure at the C=O group of the 2OP form. In view of the results obtained for 4-OH-pyridine,⁴ one expects to observe a far displaced $\nu_{\text{OH}}(2\text{HP})$ mode for the closed $\text{N}\cdots\text{H}-\text{O}\cdots\text{H}-\text{O}$ system. One component of the doublet band found at $3330/3308\text{ cm}^{-1}$ is a candidate for this mode, and we will demonstrate that this indeed is the 3330 cm^{-1} band. The shift of -244 cm^{-1} is larger than the values of -201 and -212 cm^{-1} for the corresponding open $\text{O}-\text{H}\cdots\text{OH}_2$ complexes of 3-OH-pyridine and 4-OH-pyridine.⁴ This is an indication that the closed structure is present. If this is the case, the other component at 3308 cm^{-1} should be due to the $\nu^{\text{b}}\text{OH}$ mode of the H-bonded water in the $\text{N}\cdots\text{H}-\text{O}$ H-bond. The corrected value of 3318 cm^{-1} yields the relative shift value of about 0.1, which gives with $\text{PA}_{\text{N}} = 897\text{ kJ/mol}$ a point which in the N-base correlation is far above the correlation curve.⁴⁷ The $\nu^{\text{f}}\text{OH}$ mode observed below 3700 cm^{-1} ($3696-3690\text{ cm}^{-1}$) is a further indication of the presence of the closed structure. The absorption at 3414 cm^{-1} is probably due to the $\nu^{\text{b}}\text{OH}$ mode in the open $\text{N}\cdots\text{H}-\text{OH}$ structure since the corrected value (3427 cm^{-1}) yields the corrected relative shift of 0.07, which perfectly fits on the correlation curve for the N-bases for the literature-calculated PA_{N} value of 897 kJ/mol . Calculation of the cooperativity factor, A_{b} , for the closed structure yields the value of 1.4 for the $\nu^{\text{b}}\text{OH}$ mode of bonded H_2O , which is again somewhat larger than 1.37 obtained for the $\text{N}\cdots\text{H}-\text{O}\cdots\text{H}-\text{O}$ heterotrimer.⁴⁵ The cooperativity is certainly significant between the two H-bonds in the closed structure, which results in the larger shift for the ν_{OH} frequency. However, for the cyclic water trimer, $(\text{H}_2\text{O})_3$, a much larger value of 1.73 was found,⁴⁵ which was explained by a mutual fortification caused by the extra H-bond closing the cyclic trimer. In the closed H-bonded systems, such as those studied in this work, the H-bond geometry is not the ideal and this reduces the H-bond cooperativity. The situation is different when the two H-bonds occur in a more ideal, almost linear configuration. We have illustrated this point in our previous studies where we compared the closed $\text{N}\cdots\text{H}-\text{O}\cdots\text{H}-\text{O}$ complex of 2HP- H_2O with the open $\text{N}\cdots\text{H}-\text{OH}$ water complexes of pyridine² and 4-OH-pyridine.⁴ From the cooperativity factors obtained for $\text{B}\cdot 2\text{H}_2\text{O}$ complexes⁴⁵ and the $\Delta\nu_{\text{OH}}$ shifts, we can estimate the shift of the ν_{OH} in the other possible $\text{O}-\text{H}\cdots\text{OH}_2$ open structure. We obtain the shift of $244/1.11 = 220\text{ cm}^{-1}$, or the complex frequency for the H_2O mode in the open $\text{O}-\text{H}\cdots\text{OH}_2$ complex of 3354 cm^{-1} . In this region of the spectrum shown in Figure 1, one does not observe any weak, new bands. No such absorptions were also found for $\text{H}-\text{O}\cdots\text{H}-\text{OH}$. From the thermodynamic point of view, as well as from the ab initio results, formation of a closed water complex is more probable than the open complexes, either $\text{H}-\text{O}\cdots\text{H}-\text{OH}$, $\text{O}-\text{H}\cdots\text{OH}_2$, or $\text{N}\cdots\text{H}-\text{OH}$. However, formation of the latter two structures is possible when the base OH bond is rotated away from the water molecule and points toward the C_3 atom of the pyridine ring. This is probably the reason the open $\text{N}\cdots\text{H}-\text{OH}$ and $\text{O}-\text{H}\cdots\text{OH}_2$ structures are observed in the experiment whereas the open $\text{H}-\text{O}\cdots\text{H}-\text{OH}$ complex is not.

To find more support for the assignments of the modes of both the open and closed complexes of both tautomers with H_2O , tentatively derived so far, we have recorded spectra of the matrix-isolated deuterated 2HP/2OP system in water-doped Ar matrixes. These spectra are shown in Figure 2. The ν_{OD} mode of the free, deuterated base absorbs at 2640 cm^{-1} , and ν_{ND} , at 2550 cm^{-1} . This yields the ISR (isotopic ratio) values of 1.354 and 1.351, respectively. As can be seen in Figure 2, the tautomeric equilibrium is similar for the deuterated system as for

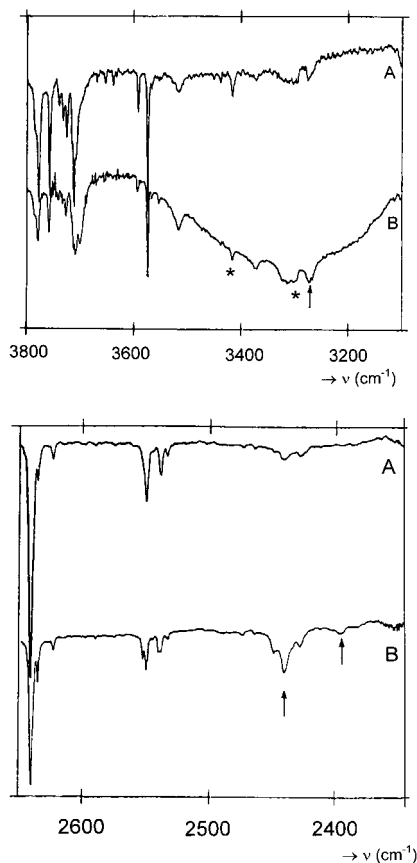


Figure 2. FT-IR spectrum of an Ar matrix doped with 2DP/2OP(D) and H₂O: (A) 2DP/2OP(D) in Ar; (B) 2DP/2OP(D)/H₂O in Ar; *, new H₂O absorption; †, new base absorption.

the nondeuterated analogue. After the water-doped matrixes were annealed, the band at 3330 cm⁻¹ almost disappears in the spectrum of the deuterated base, which allows us to interpret this band as the bonded 2HP OH mode correlated with the bonded OD mode at 2443 cm⁻¹, both being due to the shifted hydroxy mode of the base in a closed N \cdots H-O \cdots H(D)O structure. On the other hand, the bands at 3308 and 3270 cm⁻¹ remain in the spectrum of the deuterated base, which supports their assignment to the H-bonded water OH stretch in the closed complexes. The maximum of this band is situated around 3303 cm⁻¹ in the OD spectrum, which illustrates the known fact that the \cdots D-O H-bond is slightly stronger than the analogue \cdots H-O bond.⁴⁸

The complexes of the oxo tautomer of the nondeuterated base must also be observed for the deuterated base in Figure 2. Only the closed structure C=O \cdots H-O \cdots D-N should induce an additional band in the deuterated spectrum. The band observed at 2396 cm⁻¹ has an ISR value of 1.342 when correlated with the bonded H-N mode at 3210 cm⁻¹ and this supports its assignment to $\nu_{ND\cdots}$ in the closed complex of the oxo tautomer.

All the bands of the closed N \cdots H-O \cdots H-O complexes are much more intense than those of the open N \cdots H-O and O-H \cdots OH₂ complexes, which allows one to conclude that the abundance of the closed form is larger for 2HP than for 2OP.

Tautomeric Shift. Although the tautomeric equilibrium does not dramatically shift upon addition of water to the Ar matrix, some details in the spectra demonstrate that the equilibrium is slightly shifted toward the oxo form. Figure 3 illustrates this effect. The intensity of the free $\nu_{C=O}$ mode after annealing is about the same as the intensity before annealing, although two C=O complex bands appear in the latter case indicating that

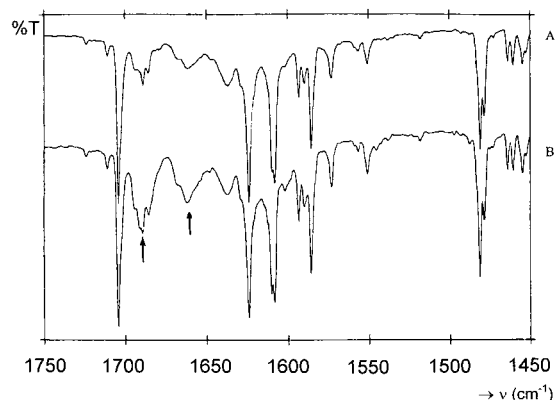


Figure 3. FT-IR spectrum of an Ar matrix doped with 2HP/2OP and H₂O: (A) before annealing; (B) after annealing. Note the intensity increase of the complex absorptions, indicated by † and a small intensity decrease of the free $\nu_{C=O}$.

more 2OP molecules formed complexes with water. This proves that the total amount of the oxo form is increased when more water is complexed by the base. This could only happen if, after formation of the N \cdots H-O \cdots H-O-C complex of 2HP, a proton transfer occurs within the H-bonded chain yielding the N-H \cdots O-H \cdots O=C complex of the 2OP form. The theoretical results listed in Table 1 support this possibility.

Comparison with Calculated Vibrational Data. For each closed complex, only the most characteristic modes have been analyzed by comparing with the calculated results. The results obtained with DFT/B3-LYP and RHF methods and the experimental matrix results are compared in Tables 4 and 5. The DFT/B3-LYP method predicts much better ν_{OH}^b and ν_{OH}^f frequencies than the RHF method. For instance, the B3-LYP ν_{OH}^b frequency for 2HP-H₂O of 3325 cm⁻¹ is close to the experimental result of 3308 cm⁻¹, while the RHF result of 3651 cm⁻¹ is much larger. Also, the best frequency shift of the ν_{OH}^b mode is obtained with the B3-LYP method. These results show that the electron correlation plays an important role in predicting the frequency shifts due to H-bonding. On the other hand, both RHF and DFT methods appear to provide reliable frequencies for $\delta(\text{HOH})$. The ν_{OH} , δ_{OH} , and γ_{OH} vibrations are the modes most perturbed by formation of the O₇-H₈ \cdots O₁₄ H-bond in 2HP-H₂O, and ν_{NH} , δ_{NH} , and γ_{NH} are most perturbed by formation of the N₁-H₇ \cdots O₁₄ bond in 2OP-H₂O. The experimental frequency shifts of the ν_{OH} and ν_{NH} modes are larger due to the cooperativity in the closed complexes, which can be explained by a larger elongation of the OH and NH bonds in these complexes. Here also the agreement between the DFT and experimental results is reasonable. For the δ_{OH} and δ_{NH} modes, both RHF and DFT predict reliable frequencies. No experimental data are available for the γ_{OH} and γ_{NH} modes. Further evidence contributing to the analysis of the H-bonding in 2HP-H₂O is obtained from calculations of shifted bending and out-of-plane OH modes equal to +27 and +157 cm⁻¹, respectively. These shifts are not larger than those obtained with the same calculation method for similar modes in the 3- and 4-hydroxypyridine open complexes.⁴ One could argue that these shifts are not in accordance with the expected larger shift values due to the cooperativity effects. As noted in the structure analysis presented in the previous section, the distortion from the perfect alignment reduces the H-bond cooperativity. This effect is also present in 2-hydroxypyrimidine-H₂O.¹ For the other modes, one notices a slightly better prediction of the frequency shifts by the DFT method. However, with a few exceptions, rather good predictions are also obtained with the RHF method.

TABLE 4: Experimental (Ar Matrix) and Calculated (B3-LYP/6-31++G and RHF/6-31++G**) Frequencies for H₂O and 2-Hydroxypyridine in the Closed Complex N···H–O···H–O**

expt: ν (cm ⁻¹)	B3-LYP ^a		RHF ^b		PED ^c	B3-LYP	RHF
	ν (cm ⁻¹)	I (km·mol ⁻¹)	ν (cm ⁻¹)	I (km·mol ⁻¹)			
	Water Modes						
3696 (–41) ^d	3881 (–46)	89	4234 (–35)	178	$\nu^f(\text{OH})$	85	88
	3687		3810		$\nu^b(\text{OH})$	17	12
3308 (–368)	3500 (–304)	1240	4057 (–89)	401	$\nu^b(\text{OH})$	87	80
	3325		3651		$\nu^f(\text{OH})$	11	15
1619 (+28)	1616 (+15)	100	1743 (+15)	124	$\delta(\text{HOH})$	76	93
	1576		1569				
561	753	181	593	133	$\delta(\cdots\text{OH H}\cdots)$	60	73
	734		534				
	Base Modes						
3330 (–244)	3400 (–369)	179	3993 (–156)	332	$\nu(\text{OH})$	75	90
	3230		3594				
1613 (+3)	1664 (+11)	111	1812 (+5)	170	$\nu(\text{C}_3\text{C}_6)$	20	23
	1622		1631		$\nu(\text{C}_2\text{C}_3)$	20	18
					$\nu(\text{C}_3\text{C}_4)$	12	12
1370 (+24)	1418 (+49)	111	1503 (+27)	65	$\delta(\text{OH})$	39	43
	1383		1353		$\delta(\text{C}_6\text{H})$	21	30
					$\delta(\text{C}_4\text{H})$	16	13
1305 (+6)	1349 (+19)	73	1459 (+13)	74	$\nu(\text{CO})$	37	40
	1315		1313		$\nu(\text{C}_3\text{C}_4)$	15	11
					δ_R	11	
?	837 (+285)	161	750 (+157)	213	$\delta(\text{C}_3\text{H})$	10	
?	820		675		$\gamma(\text{OH})$	76	86

^a First row: unscaled values. Second row: scaling factor 0.950 for $\nu(\text{XH})$, 0.980 for γ , and 0.975 for other vibrational modes. ^b First row: unscaled values. Second row: uniform scaling factor 0.900. ^c Only contributions > 10 are listed. ^d Numbers between parentheses correspond to the frequency shift.

TABLE 5: Experimental (Ar matrix) and Calculated (B3-LYP/6-31++G and RHF/6-31++G**) Frequencies for H₂O and 2-Oxopyridine in the Closed Complex C=O···H–O···H–N**

expt	B3-LYP ^a		RHF ^b		PED ^c	B3-LYP	RHF
	ν (cm ⁻¹)	I (km·mol ⁻¹)	ν (cm ⁻¹)	I (km·mol ⁻¹)			
	Water Modes						
3700 (–37) ^d	3890 (–37)	79	4237 (–32)	151	$\nu^f(\text{OH})$	82	86
	3696		3813		$\nu^b(\text{OH})$	17	13
3270 (–406)	3478 (–326)	902	4007 (–139)	278	$\nu^b(\text{H})$	89	85
	3304		3606		$\nu^f(\text{OH})$	12	12
1614 (+23)	1619 (+18)	356	1751 (+23)	321	$\delta(\text{HO H})$	99	93
	1579		1576				
	742	238	628	203	$\delta(\cdots\text{O HH}\cdots)$	85	81
	723		565				
	Base Modes						
3210 (–228)	3400 (–205)	113	3779 (–84)	264	$\nu(\text{NH})$	84	99
	3230		3401				
1691 (–13)	1736 (–17)	552	1897 (–23)	894	$\nu(\text{CO})$	39	48
	1693		1707		$\delta(\text{NH})$	17	13
					$\nu(\text{C}_2\text{C}_3)$	12	
1623 (+0)	1665 (+1)	32	1826 (+1)	60	$\nu(\text{C}_5\text{C}_6)$	35	35
	1623		1643		$\nu(\text{C}_3\text{C}_4)$	14	17
					$\delta(\text{C}_6\text{H})$	11	11
					$\delta(\text{NH})$	11	
1480 (+17)	1505 (+13)	14	1630 (+15)	27	$\delta(\text{NH})$	27	27
	1467		1467		$\nu(\text{C}_5\text{C}_6)$	21	18
					$\nu(\text{C}_3\text{C}_4)$	14	12
					$\delta(\text{C}_6\text{H})$	13	12
?	855 (+177)	118	872 (+146)	167	$\gamma(\text{NH})$	82	84
	838		785				

^{a–d} See footnotes a–d in Table 4.

Open and Closed Complexes, Bases–H₂O. Figure 4 shows the correlation between the optimal scaling factor ($\nu^{\text{exp}}/\nu^{\text{th}}$) for the bonded water ν^b_{OH} mode and the proton affinity of the base atom involved in the H-bond. Two series of complexes are presented, a series of open N···H–O complexes and a series of closed N···H–O···H–X complexes. For the open complexes, a good correlation is obtained. For the closed complexes, only

three points are available so far and a study of more closed structures is necessary in order to obtain a more meaningful correlation curve. For each series, the optimal scaling factor decreases with increasing proton affinity (PA_N) value. This originates from an increase of the anharmonicity of the H-bonded OH stretching mode with increasing H-bond strength. In the frequency calculations the harmonic approximation is used

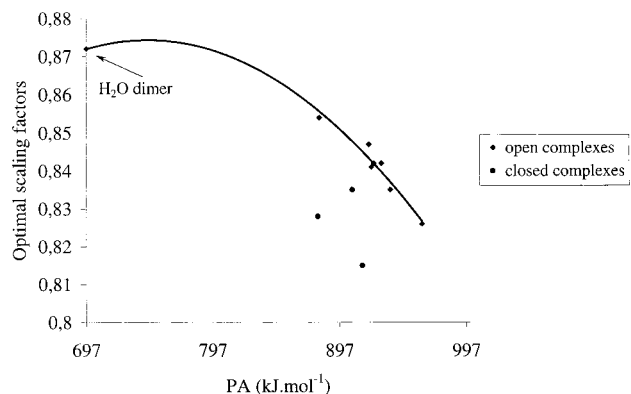


Figure 4. Correlation between the optimal scaling factor for the bonded water mode $\nu_{\text{OH}}^{\text{b}}$ and the proton affinity value of the base atom involved in the H-bond.

and the frequencies are scaled down to correct for the anharmonicity effect. For the closed complexes, larger anharmonicity scaling parameters are needed than for open complexes. This reflects larger anharmonicity than expected from the PA_{N} value, and this effect is due to the cooperativity between the two H-bonds in the closed complex. Until now, only two closed $\text{N}\cdots\text{H}-\text{O}\cdots\text{H}-\text{O}$ complexes of 2-hydroxypyrimidine¹ and 2-hydroxypyridine (this work) have been studied, but a similar observation was recently made for the closed structure of the complex hypoxanthine– H_2O .⁴⁹

Conclusion

Computational methodologies and matrix-isolation FT-IR have been used to study the H-bonding interaction of water with 2-hydroxypyridine/2-oxopyridine tautomers. On the basis of theoretical calculations (DFT and MP2), six different structures have been found. The interpretation of the IR spectra allowed identification of five strong complexes. Both theoretical and experimental methods show that the closed structures, $\text{N}\cdots\text{H}-\text{O}\cdots\text{H}-\text{O}$ and $\text{C}=\text{O}\cdots\text{H}-\text{O}\cdots\text{H}-\text{N}$, are the most stable complexes. We demonstrated with the use of the earlier established relations that a relatively strong cooperativity exists between the two bonds in the closed complexes. Also, both theory and experiment provide evidence that 2-oxopyridine interacts more strongly with a single water molecule than 2-hydroxypyridine due to the larger 2-oxopyridine dipole moment.

The rotational constants and the intermolecular distances predicted by DFT are considerably better than those obtained with the RHF method. The DFT method also yields considerably better frequencies for the modes directly involved in the H-bond.

The results obtained in this work demonstrate that the combination of matrix-isolation FT-IR with accurate computational methodologies is a suitable tool to investigate the intermolecular H-bond interactions of polyfunctional molecules modeling nucleic acid bases with water. In particular, the correlation based on the ratio between the experimental and calculated frequencies (scaling factor) and the proton affinity of the atom of the base directly involved in the H-bond allowed an analysis of the anharmonicity of the H-bonded OH stretching mode in the open and closed complexes. This information will be utilized in future interpretation of FT-IR spectra of polyfunctional bases.

References and Notes

(1) Smets, J.; Destexhe, A.; Adamowicz, L.; Maes, G. *J. Phys. Chem.* **1998**, *102*, 8157.

- (2) Destexhe, A.; Smets, J.; Adamowicz, L.; Maes, G. *J. Phys. Chem.* **1994**, *98*, 1506.
- (3) Smets, J.; Adamowicz, L.; Maes, G. *J. Phys. Chem.* **1995**, *99*, 6387.
- (4) Buyl, F.; Smets, J.; Maes, G.; Adamowicz, L. *J. Phys. Chem.* **1995**, *98*, 14967.
- (5) Smets, J.; Destexhe, A.; Adamowicz, L.; Maes, G. *J. Phys. Chem.* **1997**, *101*, 6583.
- (6) Smets, J.; Maes, G.; Adamowicz, L. *J. Phys. Chem.* **1996**, *101*, 6434.
- (7) Held, A.; Pratt, D. W. *J. Am. Chem. Soc.* **1993**, *115*, 9708.
- (8) Matsuda, Y.; Ebata, T.; Mikami, N. *J. Chem. Phys.* **1999**, *110*, 8397.
- (9) (a) Nowak, M. J.; Szczepaniak, K.; Barski, A.; Shugar, D. *J. Mol. Struct.* **1980**, *62*, 47. (b) Czerminski, R.; Kuczera, K.; Rostkowska, H.; Nowak, M. J.; Szczepaniak, K. *J. Mol. Struct.* **1986**, *140*, 235. (c) Lapinski, L.; Czerminski, R.; Nowak, M. J.; Fulara, J. *J. Mol. Struct.* **1990**, *220*, 147.
- (10) Smets, J.; Maes, G. *Chem. Phys. Lett.* **1991**, *187*, 532.
- (11) Nowak, M. J.; Lapinski, L.; Fulara, J.; Les, A.; Adamowicz, L. *J. Phys. Chem.* **1992**, *96*, 1562.
- (12) Lapinski, L.; Fulara, J.; Nowak, M. J. *Spectrochim. Acta* **1990**, *46A*, 61.
- (13) Szczepniak, M.; Kwiatkowski, J. S.; Kubulat, K.; Szczepniak, K.; Person, W. B. *J. Am. Chem. Soc.* **1988**, *110*, 8319.
- (14) Lapinski, L.; Nowak, M. J.; Fulara, J.; Les, A.; Adamowicz, L. *J. Phys. Chem.* **1990**, *94*, 6555.
- (15) Vrancken, H.; Smets, J.; Maes, G.; Lapinski, L.; Nowak, M. J.; Adamowicz, L. *Spectrochim. Acta* **1994**, *50A*, 875.
- (16) Beak, P. *Accounts. Chem. Res.* **1977**, *10*, 186. Beak, P.; Fry, F. S.; Lee, J.; Steele, F. *J. Am. Chem. Soc.* **1976**, *98*, 171. Beak, P.; Fry, F. S. *J. Am. Chem. Soc.* **1973**, *95*, 1700.
- (17) Brown, R. S.; Tse, A.; Vederas, J. C. *J. Am. Chem. Soc.* **1980**, *102*, 1174.
- (18) Guimon, C.; Garrabe, G.; Pfister-Guillouzo, G. *Tetrahedron Lett.* **1979**, 2585.
- (19) Hatherley, L. D.; Brown, R. D.; Godfrey, P. D.; Pierlot, A. P.; Caminati, W.; Damiani, D.; Melandri, S.; Favero, L. B. *J. Phys. Chem.* **1993**, *97*, 46.
- (20) Sobolewski, A. L.; Adamowicz, L. *J. Phys. Chem.* **1996**, *100*, 3933.
- (21) Becke, A. D. *J. Chem. Phys.* **1993**, *98*, 5648.
- (22) Lee, C.; Yang, W.; Parr, R. G. *Phys. Rev.* **1988**, *B37*, 785.
- (23) Dkhissi, A.; Adamowicz, L.; Maes, G. *J. Phys. Chem.*, in press.
- (24) Dkhissi, A.; Adamowicz, L.; Maes, G. *Chem. Phys. Lett.*, in press.
- (25) Chalasinski, G.; Szczepniak, M. *Chem. Rev.* **1994**, *94*, 1723.
- (26) Frisch, M. J.; Trucks, G. W.; Schlegel, H. B.; Gill, P. M. W.; Johnson, B. G.; Robb, M. A.; Cheeseman, J. R.; Keith, T.; Petersson, G. A.; Montgomery, J. A.; Raghavachari, K.; Al-Laham, M. A.; Zakrzewski, V. G.; Ortiz, J. V.; Foresman, J. B.; Peng, C. Y.; Ayala, P. Y.; Chen, W.; Wong, M. W.; Andres, J. L.; Replogle, E. S.; Gomperts, R.; Martin, R. L.; Fox, D. J.; Binkley, J. S.; Defrees, D. J.; Baker, J.; Stewart, J. P.; Head-Gordon, M.; Gonzales, C.; Pople, J. A. *Gaussian94, Revision C.3*; Gaussian Inc.: Pittsburgh, PA, 1995.
- (27) Florian, J.; Johnson, B. G. *J. Phys. Chem.* **1994**, *98*, 3681.
- (28) G. Rauhut, G.; Pulay, P. *J. Phys. Chem.* **1995**, *99*, 3093.
- (29) Florian, J.; Leszczynski, J. *J. Phys. Chem.* **1996**, *100*, 5578.
- (30) Smets, J.; Schoone, K.; Ramaekers, R.; Adamowicz, L.; Maes, G. *J. Mol. Struct.* **1998**, *442*, 201.
- (31) Maes, G. *Bull. Soc. Chim. Belg.* **1981**, *90*, 1093.
- (32) Graindourze, M.; Smets, J.; Zeegers-Huyskens, Th.; Maes, G. *J. Mol. Struct.* **1990**, *222*, 345.
- (33) Dkhissi, A.; Houben, L.; Ramaekers, R.; Adamowicz, L.; Maes, G. *J. Phys. Chem.* **1999**, *103*, 11020.
- (34) Field, M. J.; Hillier, I. H. *J. Chem. Soc., Perkin Trans.* **1987**, *2*, 617.
- (35) Barone, V.; Adamo, C. *J. Phys. Chem.* **1995**, *99*, 15062.
- (36) Kwiatkowski, J. S.; Leszczynski, J. *J. Mol. Struct.* **1996**, *376*, 325.
- (37) Kwiatkowski, J. S.; Leszczynski, J. *J. Phys. Chem.* **1996**, *100*, 941.
- (38) Del Bene, J. E. *J. Phys. Chem.* **1994**, *98*, 5902.
- (39) Dkhissi, A.; Houben, L.; Smets, J.; Adamowicz, L.; Maes, G. *J. Mol. Struct.* **1999**, *243*, 37.
- (40) Graindourze, M.; Grootaers, T.; Smets, J.; Zeegers-Huyskens, Th.; Maes, G. *J. Mol. Struct.* **1991**, *243*, 37.
- (41) Smets, J. Ph.D. Thesis, Leuven, 1993.
- (42) Katritzky, A. R.; Szafran, M.; Stevens, J. *J. Mol. Struct. Theochem.* **1989**, *184*, 179.
- (43) Bohn, R. B.; Andrews, L. *J. Phys. Chem.* **1989**, *93*, 5684.
- (44) Huyskens, P. L. *J. Am. Chem. Soc.* **1977**, *99*, 2578.
- (45) Maes, G.; Smets, J. *J. Phys. Chem.* **1993**, *97*, 1818.
- (46) Johnson, G. L.; Andrews, L. *J. Am. Chem. Soc.* **1982**, *104*, 3043.
- (47) Maes, G.; Smets, J. *J. Mol. Struct.* **1992**, *270*, 141.
- (48) Singh, T. R.; Wood, J. L. *J. Chem. Phys.* **1969**, *50*, 3572.
- (49) Ramaekers, R.; Maes, G.; Adamowicz, L.; Dkhissi, A. Manuscript in preparation.